



Title	Composition Dependence of Microstructures formed by Phase Separation in Multi-component Silicate Glass
Author(s)	Suzuki, Masanori; Tanaka, Toshihiro
Citation	ISIJ International. 2008, 48(4), p. 405-411
Version Type	VoR
URL	https://hdl.handle.net/11094/26391
rights	© 2008 ISIJ
Note	

The University of Osaka Institutional Knowledge Archive : OUKA

<https://ir.library.osaka-u.ac.jp/>

The University of Osaka

Composition Dependence of Microstructures formed by Phase Separation in Multi-component Silicate Glass

Masanori SUZUKI and Toshihiro TANAKA

Division of Materials and Manufacturing Science, Graduate School of Engineering, Osaka University, 2-1 Yamadaoka, Suita, Osaka 565-0871 Japan.

(Received on November 19, 2007; accepted on February 1, 2008)

It has been investigated that the correlation between the phase separation and glass compositions in the $\text{SiO}_2\text{-CaO-MgO-Na}_2\text{O}$ quaternary oxide glasses. The metastable miscibility gap and the spinodal region in the quaternary system have been evaluated from Gibbs energies in the metastable liquid phase, on the assumption that the glass in slag systems could be regarded as a super-cooled liquid. The microstructures corresponding to the phase separation in the glasses have been observed using transmission electron microscopy (TEM). Thermodynamic analyses and the experimental studies revealed the existence of a metastable phase separation including spinodal decomposition in the $\text{SiO}_2\text{-CaO-MgO-Na}_2\text{O}$ system. Furthermore, it was found that the size of the decomposed microstructure depended on molar ratio of CaO to MgO in the initial glass composition.

KEY WORDS: spinodal decomposition; binodal decomposition; $\text{SiO}_2\text{-CaO-MgO-Na}_2\text{O}$ system; Gibbs energy; decomposed microstructure.

1. Introduction

Phase separation in glass represents a phenomenon in which a single glass phase separates into two or more glass phases with different compositions during heat-treatment. Previous experimental studies had revealed the occurrence of phase separation in various oxide systems.¹⁻⁷⁾ To create functional glass materials using silicate slag discharged from metallurgical processes or ash melting processes, the authors have investigated the phase separation in multi-component oxide glass which contains fundamental components in waste slag.⁸⁾ Spinodal decomposition is, for example, formed as a phenomenon of phase separation. Interconnected microstructures of two phases are formed, and porous glass is produced by dissolving one of the separated glass phases with acid solution. Since the porous glass has three-dimensionally interconnected porous structures, the glass is expected to have widespread applications, for example as filters to remove impurities in water or air. Thus, slag can be transformed into value-added functional glass materials using phase separation in oxide glass.

To generate phase separation in glass from waste slag, the composition ranges for metastable immiscibility and spinodal decomposition must be evaluated for multi-component slag systems. It is, however, difficult to predict the metastable immiscibility empirically for multi-component oxide systems such as waste slag. Therefore, it is necessary to perform a thermodynamic evaluation to determine the phase separation in multi-component oxide systems.

In a previous paper,⁸⁾ the authors attempted to predict the composition ranges for metastable phase separation and spinodal decomposition in the $\text{SiO}_2\text{-CaO-MgO-5mol\%Na}_2\text{O}$

system by calculating the composition dependence of the Gibbs energy curves in the super-cooled liquid phase. In addition, the occurrence of spinodal decomposition was confirmed in heat-treated glass at a given composition in the predicted miscibility gap.

In this study, the authors have experimentally investigated the occurrence of phase separation in glass with several molar ratios of CaO to MgO in the $\text{SiO}_2\text{-CaO-MgO-5mol\%Na}_2\text{O}$ system. The occurrence of phase separation by not only spinodal decomposition but also “binodal decomposition,” which forms particle microstructures of two glass phases, is observed by transmission electron microscopy for heat-treated glass. The experimental results are compared with the thermodynamic evaluation of the metastable miscibility gap for the quaternary system.

2. Calculation of the Metastable Miscibility Gap and Composition Range for Spinodal Decomposition⁸⁾

In this paper the possibility of phase separation including spinodal decomposition was evaluated by calculating Gibbs energies and activities of SiO_2 in the metastable liquid phase, where glass in slag systems can be regarded as super-cooled liquid phase. The Gibbs energies and activities of SiO_2 are calculated with the FactSage thermodynamic computing system including the F*A*C*T oxide databases for molten oxide systems.⁹⁾

Liquid-liquid immiscibility can generally be evaluated from the Gibbs energy curve of the liquid phase. For instance, in a binary system, the miscibility gap is determined from two points of contact on the Gibbs energy curve with a common tangent. The composition range for spinodal de-

composition, referred to as the “spinodal region” in the present paper, is obtained from two inflexion points in the Gibbs energy curve.

It has been found that many binary silicate systems have metastable miscibility gaps at high concentrations of SiO₂.³⁾ The Gibbs energy curves of the liquid phases were calculated for several binary silicate systems in a previous paper.⁸⁾ The calculated results in the previous paper showed that the Gibbs energies for these systems changes linearly in SiO₂-rich composition ranges. Therefore, it may be difficult to definitively determine the spinodal region from the inflexion points in the Gibbs energy curve for silicate systems.

Here the activity of SiO₂ in the super-cooled liquid phase is calculated with concentration of SiO₂ to definitively determine the spinodal region. In an A–B binary system, the composition range for spinodal decomposition is determined by calculating differentiation of the activity with respect to composition calculated by the following Eq. (1):

$$\frac{\partial a_B}{\partial X_B} = \frac{\exp(\mu_B / RT)}{RT} \cdot \frac{\partial \mu_B}{\partial X_B} = (1 - X_B) \frac{a_B}{RT} \cdot \frac{\partial^2 G^{\text{Mix}}}{\partial X_B^2} \dots\dots\dots(1)$$

where X_B is the mole fraction of component B and G^{Mix} represents the Gibbs energy for mixing in the liquid phase. μ_B, a_B and denote the chemical potential and activity, respectively, of component B, and are expressed by Eq. (2) with respect to the pure liquid standard state:

$$\mu_B = RT \ln a_B = G^{\text{Mix}} + (1 - X_B) \frac{\partial G^{\text{Mix}}}{\partial X_B} \dots\dots\dots(2)$$

Equation (1) indicates that the spinodal region is determined from the maximum and minimum points on the activity curve since the second composition derivative of the Gibbs energy becomes zero at its inflexion points.

The above estimation procedure for the spinodal region can easily be extended to ternary or multi-component systems if one of the separated phases is composed of a pure component. On the condition that pure component A constitutes one of the separated phases, the spinodal region in an A–B–C ternary system is evaluated by calculating activity of component A across straight lines with constant composition ratio of components B to C that correspond to tie-lines of the miscibility gap. For quaternary or multi-component systems, the spinodal region is evaluated similarly by calculating the activities of A in A–B_{1-x}C_x–D quasi-ternary systems (here x is 0 to 1).

In this paper, the metastable miscibility gap in the SiO₂–CaO–MgO–5mol%Na₂O system was calculated using the FactSage thermodynamic computing program.⁹⁾ The spinodal region in the system described above was obtained by calculating the activities of SiO₂ in SiO₂–(CaO)_{1-x}(MgO)_x–Na₂O (x is 0 to 1) quasi-ternary systems, because the calculated results of activities of SiO₂ in the super-cooled liquid phase indicated that one of the separated phases in the metastable immiscibility is regarded as pure SiO₂ metastable liquid phase.⁸⁾

Figure 1 shows the calculated results for the metastable miscibility gap and the spinodal region of the SiO₂–CaO–

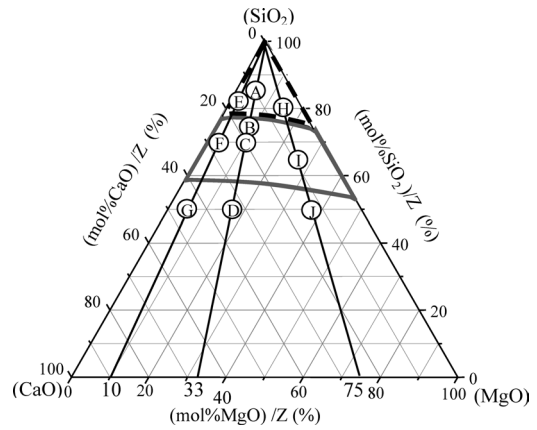


Fig. 1. Calculated composition range for phase separation in the SiO₂–CaO–MgO–5mol%Na₂O system at 948 K (dashed line: composition range for spinodal decomposition, solid line: composition range for “binodal decomposition”, Z=mol%(SiO₂+CaO+MgO)).

Table 1. Compositions of glass samples used in the experiment.

	Composition [mol%]			
	SiO ₂	CaO	MgO	Na ₂ O
A	80.8	9.5	4.7	5.0
B	71.3	15.8	7.9	5.0
C	66.5	19.0	9.5	5.0
D	47.5	31.7	15.8	5.0
E	78.4	15.0	1.6	5.0
F	66.5	25.7	2.8	5.0
G	47.5	42.8	4.7	5.0
H	75.9	4.8	14.3	5.0
I	61.8	8.3	24.9	5.0
J	47.5	11.9	35.6	5.0

MgO–5mol%Na₂O system at 948 K, where the sum of the molar concentrations of all components except Na₂O is converted to unity. Figure 1 shows that spinodal decomposition occurs in the composition range surrounded by the dotted line, and that binodal decomposition occurs in the range surrounded by the solid line.

3. Experimental Procedure

3.1. Preparation of Glass Materials

In this paper, the occurrence of phase separation is investigated for the glasses A–J, having compositions indicated by circle marks in Fig. 1, by producing two-phase glasses and observing microstructures in those glasses. The chemical compositions of glasses A–J are shown in Table 1. Silicon dioxide, magnesium oxide, sodium carbonate and calcium carbonate (all provided by Waco Corp. as special grade chemicals) were used to make these glass materials.

First, 70SiO₂–30mass%Na₂O glass was prepared as a mother glass to prevent the evaporation of Na₂O at high temperatures. Silicon dioxide and sodium carbonate were mixed in a mortar and melted in a Pt–10%Rh crucible in air for 3 h at 1373 K. The mother glass was made by quenching the melt in water. X-ray diffraction analysis was carried out on the glass using Rigaku RINT 2500V with CuKα radiation at 40 kV, 200 mA, to examine whether the sample

was glassy.

$\text{SiO}_2\text{-CaO-MgO-Na}_2\text{O}$ glasses were prepared from silica, magnesia, calcium carbonate and the $70\text{SiO}_2\text{-}30\text{mass}\%\text{-Na}_2\text{O}$ mother glass. These materials were mixed in a mortar and melted in Pt-10%Rh crucibles in air for 5 h at 1873 K. Glass samples were obtained by quenching the melts in water and examined by X-ray diffraction analysis to determine whether they were glassy or not. The glasses were then heat-treated in air for 192 h at 948 K, and then cooled to room temperature. X-ray diffraction analysis was again performed on the heat-treated glasses to confirm that they retained their glass state.

3.2. Observation of Microstructures in Heat-treated Glasses

To investigate the occurrence of phase separation, microstructures in the heat-treated glasses were observed using a transmission electron microscope HITACHI H800 with an excitation voltage of 200 kV and a camera length of 1.2 m. Preparation of the samples for electron microscopy was performed by an Ar-ion milling Gatan Model 691 with an ion-beam voltage of 4.0–4.5 kV. Some glass samples were additionally covered with carbon to prevent electrostatic charging.

4. Results and Discussion

4.1. Microstructures in Glasses with a Molar Ratio of $\text{CaO/MgO}=2/1$ (Glasses A–D)

Table 2 shows the change in the appearance of glasses A–D against holding time at 948 K. Glasses A and B turned bluish transparent with holding time. With additional time,

Table 2. Change in appearance of glasses A, B, C and D by heat treatment duration.

	Heating time [h] (Temperature: 948 K)			
	24	48	96	192
A	bluish transparent	→ adulescent	→	opalescent
B	transparent	→ bluish transparent	→	bluish transparent
C	transparent	→ transparent	→	transparent
D	transparent	→ transparent	→	transparent

glass A turned opalescent. On the other hand, glasses C and D remained transparent after heat-treatment for 192 h.

X-ray diffraction patterns for glasses A–D heated for 192 h at 948 K are shown in Fig. 2. Since crystalline peaks were not detected in the X-ray diffraction patterns, the opaqueness that appeared in glasses A and B was not attributed to crystallization of the glasses.

Figure 3 shows electron micrographs of glasses A–D heated for 192 h at 948 K, and depicts the microstructure formed by phase separation. In glass A, interconnected microstructures were observed. This structure corresponds to spinodal decomposition. The cross-section of the interconnected structure is estimated to be 80 to 100 nm in diameter. In glasses B and C, particle structures corresponding to phase separation by binodal decomposition were observed. As the composition of glass D was outside the miscibility gap, no specific microstructure was observed after heat-treatment for 192 h. Since the electron diffraction patterns for each specimen in Fig. 3 showed no evidence for the presence of crystalline phases, it was suggested that the annealed specimens were glassy in microscopic observation area.

These experimental results indicate that the microstructures observed in the heat-treated glasses can be attributed to the phase separation of glass, and that metastable liquid–liquid immiscibility occurs in glasses A–D in accordance with the thermodynamic prediction of the miscibility gap shown in Fig. 1.

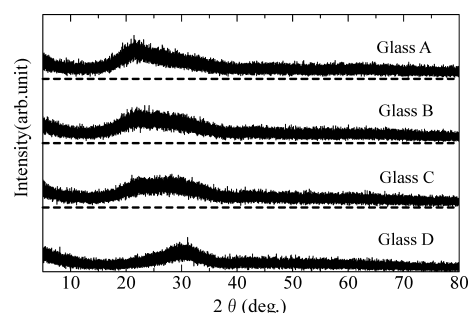


Fig. 2. XRD patterns of glasses A, B, C and D heat-treated for 192 h at 948 K.

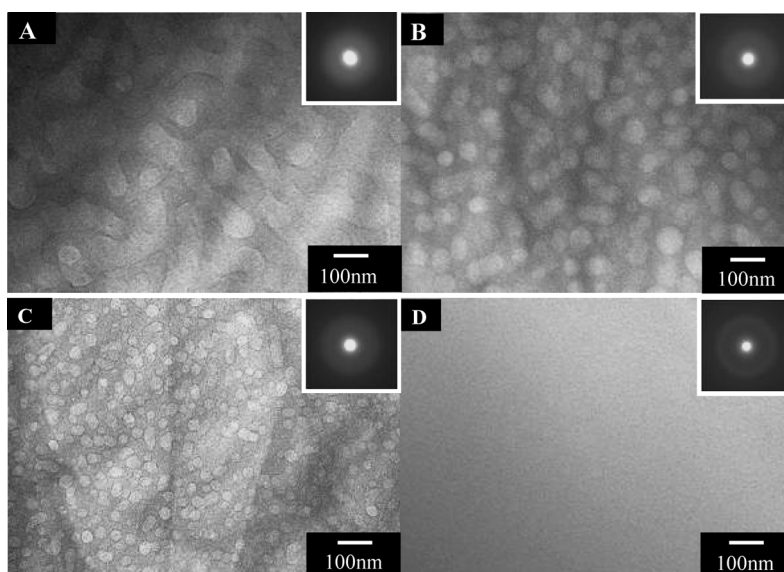


Fig. 3. Electron micrographs of glasses A, B, C and D heat-treated for 192 h at 948 K.

4.2. Microstructures in Glasses with a Molar Ratio of CaO/MgO=9/1 (Glasses E–G)

The change in the appearance of glasses E, F and G against holding time at 948 K is indicated in **Table 3**. As the holding time increased, glass E turned opaque. Glass F also turned bluish transparent and then opaque with holding time. On the other hand, glass G remained transparent after heat-treatment for 192 h.

X-ray diffraction patterns for glasses E, F and G heated for 192 h at 948 K are shown in **Fig. 4**. Since crystalline peaks are not detected in the X-ray diffraction patterns, the opaqueness that appeared in glasses E and F was not attributed to crystallization.

Electron micrographs of glasses E, F and G heated for 192 h at 948 K are presented in **Fig. 5**. Since no evidence for the presence of crystalline phases was detected in the electron diffraction patterns for each specimen in Fig. 5, it was indicated that the annealed specimens were glassy in microscopic observation area. In glass E, interconnected microstructure was observed, and the cross-section of this

Table 3. Change in appearance of glasses E, F and G by heat treatment duration.

	Heating time [h] (Temperature: 948 K)			
	24	48	96	192
E	adulescent →	opalescent →	opalescent	
F	transparent →	bluish transparent →	adulescent	
G	transparent →	transparent →	transparent	

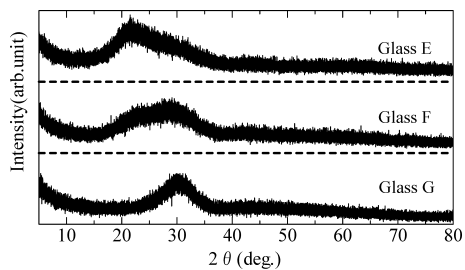


Fig. 4. XRD patterns of glasses E, F and G heat-treated for 192 h at 948 K.

structure is estimated to be 100 nm. In glass F, particle structures 50 nm in diameter were observed. This structure corresponds to phase separation by binodal decomposition. As the composition of glass G is outside the miscibility gap, no specific microstructure was observed after the heat-treatment for 192 h.

These experimental results indicate that phase separation occurs in glasses E, F and G in accordance with the thermodynamic prediction of the miscibility gap shown in Fig. 1.

4.3. Microstructures in Glasses with a Molar Ratio of CaO/MgO=1/3 (Glasses H–J)

Table 4 summarizes the change in the appearance of glasses H, I and J against holding time at 948 K. Glass H turned slightly bluish transparent as holding time increased. Glasses I and J, however, remained transparent after heat-treatment for 192 h.

Figure 6 shows X-ray diffraction patterns for glasses H, I and J heated for 192 h at 948 K. Since crystalline peaks were not detected in the X-ray diffraction patterns, the

Table 4. Change in appearance of glasses H, I and J by heat treatment duration.

	Heating time [h] (Temperature: 948 K)			
	24	48	96	192
H	transparent →	transparent →	bluish transparent	
I	transparent →	transparent →	transparent	
J	transparent →	transparent →	transparent	

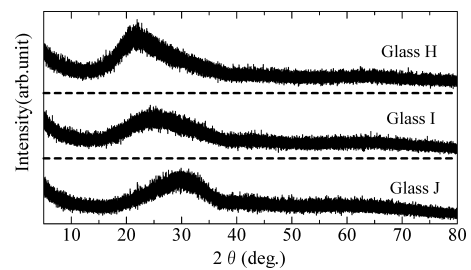


Fig. 6. XRD patterns of glasses H, I and J heat-treated for 192 h at 948 K.

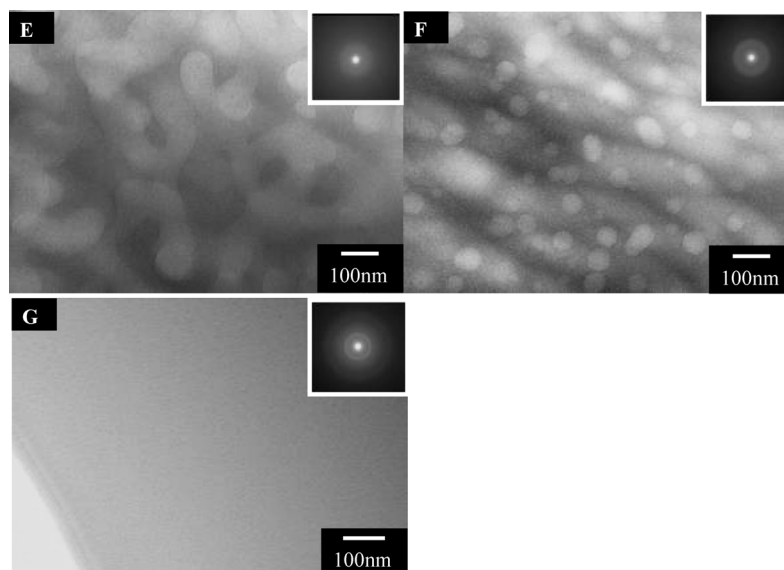


Fig. 5. Electron micrographs of glasses E, F and G heat-treated for 192 h at 948 K.

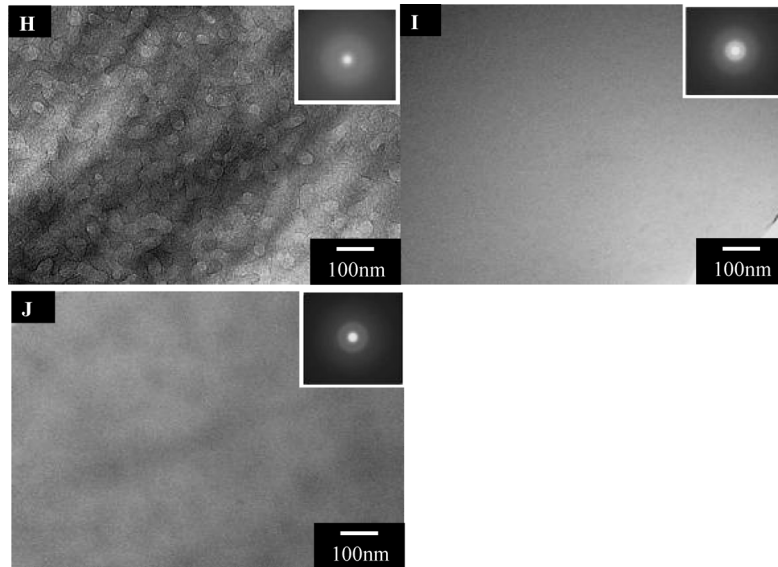


Fig. 7. Electron micrographs of glasses H, I and J heat-treated for 192 h at 948 K.

opaqueness that appeared in glass I was not attributed to crystallization.

Electron micrographs of glasses H, I and J heated for 192 h at 948 K are shown in Fig. 7. Since the electron diffraction patterns for each specimen in Fig. 7 showed no evidence for the presence of crystalline phases, it was indicated that the annealed specimens were glassy in microscopic observation area. In glass H, interconnected microstructures corresponding to spinodal decomposition were observed. The cross-section of this modulated structure is estimated to be 40 nm. Although the composition of glass I was in the predicted miscibility gap, no specific microstructure was observed in glasses I and J after heat-treatment for 192 h.

4.4. Composition Dependence of Phase Separation in SiO₂-CaO-MgO-Na₂O Oxide Glass

Table 5 summarizes the above experimental results for microstructures formed by the glass-glass immiscibility. In this table, the solid circles denote the glass compositions in which spinodal decomposition was confirmed, the double circles denote the binodal decomposition, and the open circles show where the occurrence of phase separation was not observed in the heated glasses with the relevant composition. The cross-section or size of these microstructures in the glass samples heated for 192 h at 948 K is also given in this table. Table 5 shows that the size of the decomposed microstructures in glasses decreases as concentration of SiO₂ decreases where the molar ratio of CaO/MgO is constant. It also shows that the spinodal decomposition forms larger microstructures than those for binodal decomposition. It should be noted that spinodal decomposition is yielded immediately by infinitesimal composition fluctuation, although binodal decomposition is developed through nucleation of another glass phase. Therefore, the decomposed microstructure in the spinodal decomposition is expected to be developed more rapidly than that in the binodal decomposition.

In addition, Table 5 suggests that the size of the microstructures in the glasses decreases as the molar ratio of

Table 5. Composition dependence of microstructures formed by phase separation in glasses (heat-treatment conditions: 948 K, 192 h).

●:Spinodal decomposition; ⊙:Binodal decomposition; ○:No immiscibility)

CaO/MgO molar composition ratio	Mole fraction of SiO ₂			
	1.00	0.80	0.60	0.40
90/10	← Spinodal decomposition ← Binodal decomposition → →			
90/10		E (●)	F (⊙)	G (○)
		100nm	50nm	
67/33		A (●)	B (⊙)	C (⊙)
		80-100nm	50nm	30nm
25/75		H (●)	I (○)	J (○)
		40nm		

CaO/MgO decreases under a given heat-treatment conditions (948 K, 192 h). Consequently, it has been found that the size of microstructures produced by phase separation can be controlled by manipulating the initial compositions of glasses, as well as the thermal conditions of heat-treatments. Although phase separation is expected in annealed glass I, the microstructures in this glass are considered to be too small to be detected in the electron microscopic observation.

In the case of the spinodal decomposition, the reason why the size of decomposed microstructure depends on the molar ratio of CaO/MgO in initial glass composition is discussed below. According to the theory proposed by Cahn *et al.*,¹⁰⁾ the development of microstructure by spinodal decomposition is analyzed by the summation of sinusoidal waves of mass transfer with fixed wavelength and random direction or amplification, and then the wavelength of the composition fluctuation is expressed by the following equation:

$$\lambda_m = 4\pi / \left(- \frac{1}{\kappa} \frac{\partial^2 G^{Mix}}{\partial X_B^2} \right) \dots\dots\dots(3)$$

where κ represents the composition gradient energy coefficient and corresponds to the interfacial excess energy at

the phase boundary of decomposed microstructures. The second composition derivative of the Gibbs energy in Eq. (3) represents the driving force of the spinodal decomposition. Therefore, the size of decomposed microstructure is expected to be determined from the driving force of the spinodal decomposition and the interfacial excess energy of decomposed phases.

As expressed in Eq. (1), the second composition derivative of the Gibbs energy is proportional to the first differentiation of the activity with respect to composition. To investigate the effect of the driving force of the spinodal decomposition on the size of microstructure, the composition dependence of activities of SiO_2 in the super-cooled liquid phase were evaluated for the SiO_2 -CaO-MgO system and presented in Fig. 8. In this figure, the activities of SiO_2 were calculated with concentrations of SiO_2 for constant molar ratio of CaO/MgO. On the condition that one of decomposed phases is regarded as pure SiO_2 metastable liquid phase, the spinodal region is determined from the composition range where the gradient of the activity with respect to composition is negative. Then, the driving force of the spinodal decomposition is estimated from the gradient of the activity of SiO_2 with respect to composition. Since the gradients of the activities of SiO_2 in the spinodal region are comparable for any molar ratios of CaO/MgO as

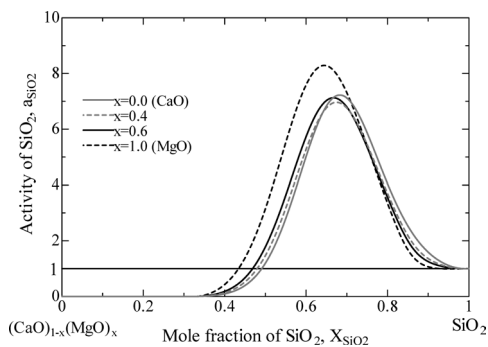


Fig. 8. Calculated results of activities of SiO_2 in the SiO_2 -CaO-MgO system at 948 K.

shown in Fig. 8, the driving force of spinodal decomposition is not considered to be dominant for the dependence of the molar ratio of CaO/MgO on the size of the microstructure.

On the other hand, Eq. (3) suggests that the spinodal wavelength λ_m can change with the interfacial excess energy κ when κ has composition dependence in silicate glass. For example, λ_m increases with increasing κ , and consequently the size of the microstructure is expected to increase in order to minimize integral interfacial area. Thus, the effect of the molar ratio of CaO/MgO on the size of the microstructure might be determined from the composition dependence of κ in the silicate glass investigated in this paper. However, since the exact information has not been accumulated on the composition dependence of κ in silicate glass materials, we can not explain the detail correlation of the size of the microstructure in the spinodal decomposition with the composition dependence of κ at the present stage. The primary factor to dominate the size of the decomposed microstructure should be investigated continuously.

4.5. Development of Microstructures during Observation with a Transmission Electron Microscope

In several annealed glasses investigated in this study, a dynamic development of microstructures was observed with a transmission electron microscope. Figure 9 represents electron micrographs of glass I heat-treated for 192 h at 948 K, showing the effect of observation time under electron microscopy. As shown in Figs. 9(1)–9(4), particle microstructure was generated and each particle expanded in the glass matrix during 25 min of electron microscopy, even though no specific microstructure was observed in the glass after heat-treatment. Consequently, it was concluded that the microstructure of heat-treated glasses can expand during electron microscopic observation. The dynamic development of microstructure during microscopic observation was also indicated for heated glass J, as shown in Fig. 10. Stereo microphotography of the microstructure in glass I

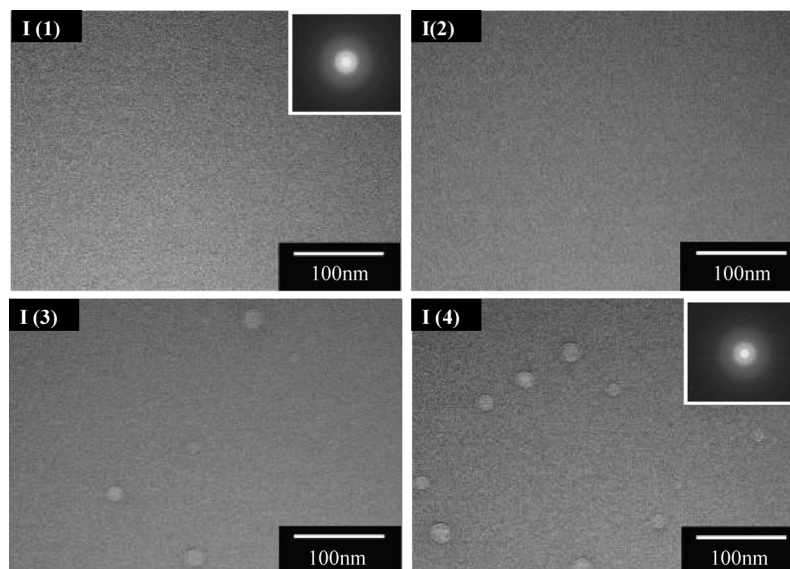


Fig. 9. Electron micrographs of heat-treated glass I showing the effect of observation time on the microstructure of the glass: (1) initial structure, (2) structure after 10, (3) 20, (4) 25 min of observation by electron microscopy. (heat-treatment conditions: 948 K, 192 h).

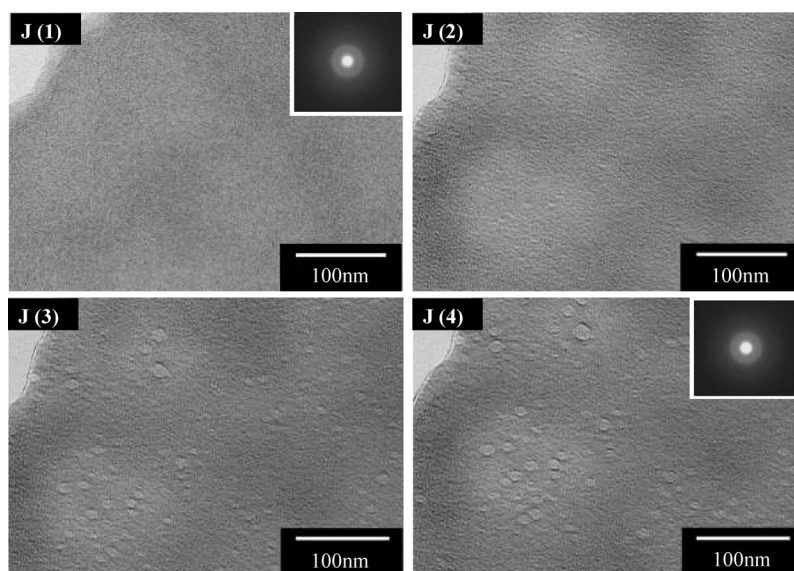


Fig. 10. Electron micrographs of heat-treated glass J showing the effect of observation time to change microstructure in glass: (1) initial structure, (2) structure after 10, (3) 20, (4) 25 min of observation by electron microscopy. (heat-treatment conditions: 948 K, 192 h).

revealed that the particle structures in the observation area expanded three-dimensionally.

Since crystalline spots or rings were not detected in the result of electron diffraction patterns for the glasses I and J after microscopic observation, the dynamic development of the particle microstructures was not attributed to the formation of a nano-crystalline phase. It is considered that the particle structure described above develops due to the phase separation by binodal decomposition which is accelerated by electron beam irradiation and local defect formation at the observation area. It should be noted that the decomposed microstructures observed in heated glasses A, B, C, E, F, and H were not attributed to the dynamic development of microstructures under electron microscopy, because those microstructures were found throughout the observation area in the glasses after heat-treatment.

5. Conclusions

The occurrence of phase separation in the SiO_2 -CaO-MgO- Na_2O system was investigated by observing microstructures in heat-treated glasses with transmission electron microscopy. The composition dependence of the change in microstructures of two-phase glass was compared with the metastable miscibility gap and spinodal region. These were evaluated from thermodynamic analyses on the assumption that glass in the oxide system described above can be regarded as a super-cooled liquid phase.

Experimental studies in this paper indicate that the morphology of the glass microstructures changes from interconnected structures by spinodal decomposition, to a particle structure by binodal decomposition, as concentration of SiO_2 decreases under a fixed molar ratio of CaO to MgO. This correlation, between the occurrence of phase separation and initial glass compositions, corresponds to the calculated metastable miscibility gap and spinodal region. Consequently it was found that the possibility of glass-glass immiscibility can be evaluated from thermodynamic analyses on Gibbs energy for the metastable liquid

phase for multi-component silicate systems.

The size of the microstructures formed by the phase separation depends on the molar ratio of CaO to MgO in initial glass compositions. In particular, fine microstructures are observed in glasses with low molar ratios of CaO to MgO.

Acknowledgements

This study was supported by Priority Assistance for the Formation of Worldwide Renowned Centers of Research—The Global COE Program (Project: Center of Excellence for Advanced Structural and Functional Materials Design) from the Ministry of Education, Culture, Sports, Science and Technology (MEXT), Japan.

Observation of the microstructures in the samples by transmission electron microscopy was also supported by professor Hakasetaro Mori and technical official Eiji Taguchi (Research center for Ultra-high voltage electron microscopy, Osaka University), and carried out in a facility in the Research center for Ultra-high voltage electron microscopy, Osaka University. We thank them most warmly for their assistance in this study.

REFERENCES

- 1) Y. Utsumi, S. Sakka and M. Tashiro: *Glass Technol.*, **11** (1970), 80.
- 2) D. G. Burnett and R. W. Douglas: *Phys. Chem. Glasses*, **11** (1970), 125.
- 3) W. Haller, D. H. Blackburn and J. H. Simmons: *J. Am. Ceram. Soc.*, **57** (1974), 120.
- 4) T. P. Seward, D. R. Uhlmann and D. Turnbull: *J. Am. Ceram. Soc.*, **51** (1968), 278.
- 5) B. S. R. Sastry and F. A. Hummel: *J. Am. Ceram. Soc.*, **42** (1959), 81.
- 6) P. Taylor and D. G. Owen: *J. Am. Ceram. Soc.*, **64** (1981), C-158.
- 7) W. Haller, D. H. Blackburn, F. E. Wagstaff and R. J. Charles: *J. Am. Ceram. Soc.*, **53** (1970), 34.
- 8) M. Suzuki and T. Tanaka: *ISIJ Int.*, **46** (2006), 1391.
- 9) C. W. Bale, A. D. Pelton, W. T. Thompson and G. Eriksson: Fact-Sage, Ecole Poly-technique, Montreal, (2001), <http://www.crct.polymtl.ca>. (Accessed on 5th, October, 2007)
- 10) J. Cahn: *J. Chem. Phys.*, **24** (1956), 93.